

Cite this: *RSC Adv.*, 2018, 8, 8080

N*-Acetyl-L-leucine-polyethylenimine-mediated miR-34a delivery improves osteogenesis and bone formation *in vitro* and *in vivo

Yubin Shen,^a Yin Liu,^a Han Gao,^a Hongbo Fei,^a Wenwen Yu,^b Tianqi Hu,^a Yi Zheng,^a Xueting Bi^a and Chongtao Lin^{*a}

Oral bone defects are difficult to treat. Recently, endogenous miR-34a was shown to be involved in bone anabolism. Clinical application of such microRNAs requires the inherent instability of microRNAs to be overcome by an efficient delivery system. In this study, we employed *N*-acetyl-L-leucine-modified polyethylenimine (*N*-Ac-L-Leu-PEI) as an miR-34a carrier and evaluated its delivery ability, transfection efficiency, cytotoxicity and whether it enhanced osteogenic differentiation and bone formation *in vitro* and *in vivo*. Stable *N*-Ac-L-Leu-PEI/miR-34a nanocomplexes were synthesized at a mass ratio of 4 and had a small size (190.34 nm), a low zeta potential (21.1 mV), a high transfection efficiency (69.39%) and no cytotoxicity in MG63 cells. *N*-Ac-L-Leu-PEI-mediated miR-34a delivery *in vitro* promoted ALP activity and expression of osteogenic differentiation markers, *Runx2*, *SP7* and *Coll* to higher levels than those produced by Lipofectamine 2000-mediated delivery. *N*-Ac-L-Leu-PEI also achieved delivery of miR-34a *in vivo* to a local cranial bone defect area with miR-34a retaining the ability to initiate significant new bone formation 12 weeks post-implantation. This demonstrates the potential for *N*-Ac-L-Leu-PEI as a gene therapy vehicle for the regeneration of bone defects.

Received 18th November 2017

Accepted 12th February 2018

DOI: 10.1039/c7ra12548h

rsc.li/rsc-advances

1. Introduction

Defects in oral bones are serious sequelae of tumors, periodontitis, fractures and surgery, and the ultimate goal of complete bone tissue regeneration after injury is still a great challenge. Various therapeutic methods have been applied, such as bone transplantation, guided bone regeneration, bone replacement technology, and tissue engineering; however, all these strategies have limitations.¹ To improve these methods, many studies have recently applied gene therapy to bone regeneration.

miR-34a is regarded as an efficient regulator of bone metabolism.^{2–6} miR-34a is an evolutionarily conserved miRNA and is an endogenous inhibitor of osteoclasts to block osteoporosis and bone metastasis by suppressing osteoclastogenesis and Tgfr2.⁴ miR-34a is also implicated in tooth development, being expressed during various stages of tooth growth, and regulates the differentiation and proliferation of human dental papilla cells.^{7,8} The effects of miR-34a on osteogenic differentiation are multiple. miR-34s inhibit osteogenic proliferation and differentiation in mice,⁵ but miR-34a plays a positive role in osteogenesis and bone formation in human adipose-derived

stromal cells⁶ via the RBP2/NOTCH1/CYCLIN D1 core regulatory network. From these findings it was suggested that gene therapy based on miR-34a could be a valuable approach to achieve bone regeneration. However, microRNA instability and low intracellular penetration limited its application in bone tissue regeneration.⁹ It is, therefore, necessary to apply an effective delivery system for miR-34a-mediated gene therapy.

Non-viral carriers, such as cationic polymers polyethylenimine (PEI) and cyclodextrin, are regarded as “gold standard” delivery systems due to their high gene-loading capacity, low production cost and low immunogenicity.^{10–12} Branched PEI, with an average molecular weight of 25 kDa (PEI25K), exhibits high gene transfection efficiency owing to its high cationic density. This characteristic also promotes condensation of nucleic acids into polyplexes and facilitates their transfer into cells and endosome release.^{13,14} However, the excessive positive charge of PEI25K can also cause cytotoxicity and hemolysis as well as serum instability.^{15,16} To solve these problems, PEI25K has been chemically modified by grafting hydrophobic groups or polymers to enhance transfection efficiency and to decrease cytotoxicity.^{17–19} In a previous study, the derivative *N*-acetyl-L-leucine-modified polyethylenimine (*N*-Ac-L-Leu-PEI) was constructed by grafting hydrophobic *N*-acetyl-L-leucine onto PEI25K, and the carrier improved transfection efficiency and biocompatibility. This carrier has been successfully applied in delivery of the p53 gene²⁰ and a DNase²¹ to inhibit the proliferation and migration of tumor cells.

^aDepartment of Periodontics, School and Hospital of Stomatology, Jilin University, 1500 Qinghua Road, Changchun 130021, China. E-mail: linct@jlu.edu.cn; Tel: +86-431-88796039

^bDepartment of Orthodontics, School and Hospital of Stomatology, Jilin University, 1500 Qinghua Road, Changchun 130021, China



In this study, *N*-Ac-L-Leu-PEI was employed as a carrier for miR-34a to investigate whether *N*-Ac-L-Leu-PEI could effectively deliver miR-34a without toxicity so as to regulate osteogenesis *in vitro* and *in vivo*. The characteristics of *N*-Ac-L-Leu-PEI/miR-34a were determined by gel retardation, particle size and zeta potential assays. Transfection efficiency and cytotoxicity were detected by flow cytometry and MTT assays. Finally, the miR-34a regulation of osteogenic differentiation of MG63 cells *in vitro* and of bone regeneration in a cranial bone defect model *in vivo* was evaluated.

2. Materials and methods

2.1 Materials

The miR-34a mimics and FAM-labeled miR-34a were synthesized by Gene Pharma (Suzhou, China): miR-34a, sense: 5'-AGCCGCTGGCAGTGTCTTA-3'; antisense: 5'-CAGAGCAGGGTCC-GAGGTA-3'. The derivative *N*-Ac-L-Leu-PEI was constructed according to a previous report²⁰ and branched PEI25K (Sigma-Aldrich, St. Louis, USA) was provided by the School of Life Sciences, Jilin University. Lipofectamine 2000 was purchased from Invitrogen. Dulbecco's Modified Eagle's Medium (DMEM), fetal bovine serum (FBS) and trypsin were purchased from Hyclone (Hyclone, USA). 3-(4,5-dimethylthiazol-2-yl)-2,5-diphenyltetrazolium bromide (MTT) was sourced from Sigma (USA). The annexin V-FITC/propidium iodide (PI) apoptosis detection kit was purchased from Shenggong (Shanghai, China). The PrimeScript™ RT reagent kit and SYBR-Green premix ExTaq™ were purchased from Takara (Dalian, China). All other chemicals used were of the highest reagent grade commercially available and used as received. The following instruments were used: Olympus IX71 fluorescence microscope (Olympus, Japan), microplate reader (Rayto, USA), FACSCalibur (BD Bioscience, Mountain View, USA), NanoDrop 1000 spectrophotometer (Thermo Scientific, USA), and Mx3005P fluorescence quantitative PCR instrument (Agilent Technologies, USA).

2.2 Gel retardation assay

N-Ac-L-Leu-PEI/miR-34a nanocomplexes were prepared at different mass ratios by incubation at room temperature for 30 minutes. The ability of *N*-Ac-L-Leu-PEI to bind to miR-34a was assessed by 1.5% agarose gel electrophoresis in a Tris-acetate-ethylenediaminetetraacetic acid buffer (80 V, 25 minutes).

2.3 Size distribution and zeta potential

The particle sizes and zeta potentials of *N*-Ac-L-Leu-PEI/miR-34a nanocomplexes were examined using a Zetasizer Nano ZS90 (Malvern Instruments, Malvern, UK). The morphologies of *N*-Ac-L-Leu-PEI/miR-34a nanocomplexes were determined by transmission electron microscopy (TEM) (FEI Tecnai G2 STWINF20). These tests were repeated three times.

2.4 Flow cytometry (FCM) and fluorescence observation

The *in vitro* gene transfection efficacy of Lipofectamine 2000 and *N*-Ac-L-Leu-PEI was evaluated in MG63 cells. MG63 cells were seeded in 6-well plates at 3×10^5 cells per well²² and

cultured for 24 h prior to transfection (when they had reached 70–80% confluency). Next, the medium was replaced with serum-free medium containing polymer/FAM-miR-34a polyplexes at an miR-34a concentration of $0.1 \mu\text{g mL}^{-1}$. Six hours after transfection, cells were washed with PBS and analyzed on an Olympus IX71 fluorescence microscope (Osaka, Japan) at 480 nm. Transfection efficiency was evaluated by scoring the percentage of FAM-miR-34a⁺ cells by flow cytometry using a FACSCalibur (BD Bioscience Mountain View, USA).

2.5 Cell viability assay

The cytotoxicity of Lipofectamine 2000-, PEI25K- and *N*-Ac-L-Leu-PEI-mediated miR-34a delivery was evaluated using an MTT assay. MG63 cells were seeded into a 96-well plate at a density of 5×10^3 cells per well and pre-incubated at 37 °C in 5% CO₂ for 24 h. Cells were then cultured with polymer/miR-34a nanocomplex at a mass ratio of 4 : 1. After co-culture for 24, 48 or 72 h, 20 μL MTT solution (1 mg mL⁻¹ in PBS) was added to each well and the plate was incubated for an additional 4 h. After removing the MTT solution, 150 μL per well DMSO was added to dissolve the formazan crystals. Following an additional incubation for 10 min, the absorbance at 492 nm was recorded using a microplate reader (Rayto, USA). The cell viability (%) was calculated as $A_{\text{sample}}/A_{\text{control}} \times 100$.

2.6 Apoptosis and live/dead cell assays

miR-34a-induced apoptosis was analyzed using an Annexin V-FITC/PI apoptosis detection kit (Shenggong, Shanghai, China). MG63 cells were seeded in a 6-well plate at a density of 3×10^5 cells per well²² and incubated for 24 h before transfection. Transfection was performed using the PEI25K or *N*-Ac-L-Leu-PEI/miR-34a nanocomplex (4 wt/wt ratio, 2 μg miR-34a) in serum-free DMEM for 6 h. After incubation in DMEM containing 10% FBS for 72 h, cells were harvested, washed twice with PBS and resuspended in binding buffer according to the manufacturer's protocol. Cells were then incubated with Annexin V-FITC/PI at room temperature for 20 min in the dark. Apoptosis was assessed by analyzing 10 000 cells gated through a FACSCalibur (BD Biosciences) with Cell Quest software (BD Biosciences).

Transfected MG63 cells for live/dead cell assays were washed with PBS and then incubated with Calcein-AM/PI at room temperature for 30 min in the dark. Cell images were collected under blue-ray and green-ray to calculate the percentage of cells.

2.7 Real-time PCR assay

MG63 cells were harvested after incubation with *N*-Ac-L-Leu-PEI/miR-34a or Lipofectamine 2000/miR-34a for 72 h. RNAs were isolated using a HiPure Total RNA kit (Magen, China) according to the manufacturer's instructions. miRNA was subjected to reverse transcription and PCR using a SYBR Green Hairpin-it miRNAs qRT-PCR kit. mRNAs were also reverse transcribed and amplified using a PrimerScript® RT reagent kit and SYBR Green Premix Ex Taq. The PCR products were evaluated with an MxPro Mx3005P real-time PCR detection system (Agilent Technologies, Santa Clara, CA, USA). The internal controls of mRNAs and miR-34a were GAPDH and U6, respectively. The cycling



conditions of mRNAs were: 95 °C for 30 s, followed by 40 cycles of 95 °C for 5 s, 55 °C for 30 s, and 72 °C for 1 min. The cycling conditions for miRNAs were: 95 °C for 3 min, followed by 40 cycles of 95 °C for 12 s, and 62 °C for 40 s. The $2^{-\Delta\Delta C_t}$ method was used to calculate relative expression levels, and the obtained values were the average of triplicate measurements. Primers used for qPCR were:

U6, F:5'-ATTGGAACGATACAGAGAAGATT-3'/R:5'-GGAACGCTTCACGAATTTG-3'; miR-34a, F:5'-AGCCGCTGGCAGTGTCTTA-3'/R:5'-CAGAGCAGGGTCCGAGGTA-3'.

GAPDH, F:5'-ACCACAGTCCATGCCATCAC-3'/R: 5'-TCCACACCCTGTTGCTGTA-3'; Runx2, F:5'-TTGCAGTCTTCCTGGA GAAAGTT-3'/R:5'-CCTCTCGACCCGACTGCAGATC-3';

SP7, F:5'-CACAGCTCTTCTGACTGTCTG-3'/R:5'-CTGGTGA AATGCCTGCATGGAT-3';

COL-1, F:5'-AGGGCCAAGACGAAGACATC-3'/R:5'-AGAT CACGTCATCGCACAAACA-3'.

2.8 Western blot analysis

The effect of miR-34a transfection on the expression of proteins associated with osteoblast-related factors was evaluated by western blotting, in which protein levels were normalized against those of GAPDH. Seventy-two hours after transfection with the *N*-Ac-L-Leu-PEI/miR-34a nanocomplex (4 wt/wt ratio, 2 µg miR-34a), MG63 cells were harvested, washed twice with ice-cold PBS and lysed with RIPA lysis buffer on ice for 5 min. The lysates were centrifuged at $14\,000 \times g$ for 15 min and supernatants collected. Protein concentrations were determined using a BCA protein assay kit. Equal amounts of protein were subjected to SDS-PAGE and subsequently transferred to PVDF membranes by electroblotting. The membranes were blocked in PBS containing 5% skimmed milk and 0.1% Tween-20 for 1 h, and then incubated with desired antibodies at 4 °C overnight. Membranes were subsequently incubated with an HRP-goat anti-rabbit IgG (H + L) antibody for 1 h and detected using enhanced chemical luminescence (Amersham, UK).

2.9 Rat cranial bone defect model

All animal procedures were approved by the International Animal Care and Use Committee of Jilin University, Changchun, People's Republic of China. The animal experiments were performed in accordance with the requirements of the Experimental Animal Ethics and Welfare guidelines (Permit Number: 20160205). Eight-week-old male Wistar rats with an average weight of 180 g were obtained from the Animal Experiment Center of Jilin University. The bone defect model was prepared according to Yin²³ and Zhao.²⁴ Rats were anesthetized using ketamine (60 mg kg⁻¹) and xylazine (8 mg kg⁻¹). The experimental area was shaved and sterilized and the scalp tissue separated along the midline to expose the calvarias area. Unilateral critical bone defects (6 mm in diameter) were created using a bone trephine (3i Implant Innovation, Palm Beach Gardens, FL, USA). The *N*-Ac-L-Leu-PEI/miR-34a and Lipofectamine 2000/miR-34a nanoparticles were synthesized with 2 µg miR-34a at a W/W ratio of 4 : 1, and were then

absorbed into a 5 mm diameter, 1.5 mm thick gelatin sponge. The gelatin sponge covered the defect area, and stratified suture wound. The experimental rats were sacrificed at 12 weeks after implantation and exsanguinated *via* the auricula dextra and perfused *via* the ventriculus dexter using 4% paraformaldehyde solution. Cone Beam Computerized Tomography (CBCT) and Microcomputed tomography (micro-CT) (micro-CT 35; Scanco Medical AG, Bassersdorf, Switzerland) was used to evaluate new bone formation. Quantification of new bone formation was calculated using Image-Pro Plus software.

2.10 Statistical analysis

Experiments were performed on at least three individuals. Results are presented as the mean \pm standard deviation and were statistically analyzed with Student's *t*-test unless noted otherwise. A two-tailed *P*-value of <0.05 was considered statistically significant. *P* values were **P* < 0.05, ***P* < 0.01, and ****P* < 0.001, with n.s. (non-significant) *P* > 0.05. Statistical analysis was conducted in SPSS version 20.0 (IBM).

3. Results

3.1 Characterization of the *N*-Ac-L-Leu-PEI/miR-34a nanocomplex

The binding of *N*-Ac-L-Leu-PEI and miR-34a was assessed using an agarose gel retardation assay. Partial to complete binding was observed between *N*-Ac-L-Leu-PEI and miR-34a at a mass rate of 2 (Fig. 1A), indicating the formation of a stable *N*-Ac-L-Leu-PEI/miR-34a complex. Compared with plasmid DNA (critical mass rate of 0.6–0.8),²⁰ *N*-Ac-L-Leu-PEI exhibited lower binding ability for microRNAs and single-stranded oligoDNAs (critical mass rate of 2.0).²¹ The ability of PEI to condense DNA constructs into nanocomplexes and to decrease their negative charge prevents them from escaping from lysosomes, promoting their delivery into cells.^{13,14} We examined the particle size and zeta potential of *N*-Ac-L-Leu-PEI/miR-34a nanocomplexes at different mass ratios (Fig. 1B and C). The size of *N*-Ac-L-Leu-PEI/miR-34a complexes rapidly declined with an increasing w/w ratio (Fig. 1B). The smallest *N*-Ac-L-Leu-PEI/miR-34a complex was 190.34 ± 6.76 nm at a mass ratio of 4 : 1. The zeta potential also decreased with increasing w/w ratio, with the lowest being 12.93 ± 1.67 mV at a 6 w/w ratio (Fig. 1C). TEM images of *N*-Ac-L-Leu-PEI/miR-34a complexes showed a globular morphology with an average size of approximately 200 nm (Fig. 1D). This indicated that *N*-Ac-L-Leu-PEI was able to form stable nanoparticles with miR-34a.

3.2 Transfection efficiency of *N*-Ac-L-Leu-PEI/miR-34a

The derivative *N*-Ac-L-Leu-PEI has achieved successful delivery of the p53 gene and a DNAzyme with higher transfection efficiency compared with PEI25K and Lipofectamine 2000.^{20,21} To determine whether *N*-Ac-L-Leu-PEI can achieve acceptable transfection efficiency with microRNAs, we employed fluorescence microscopy, flow cytometry (FCM) and qRT-PCR. Inverted fluorescence microscopy identified FAM-miR-34a⁺ cells in both



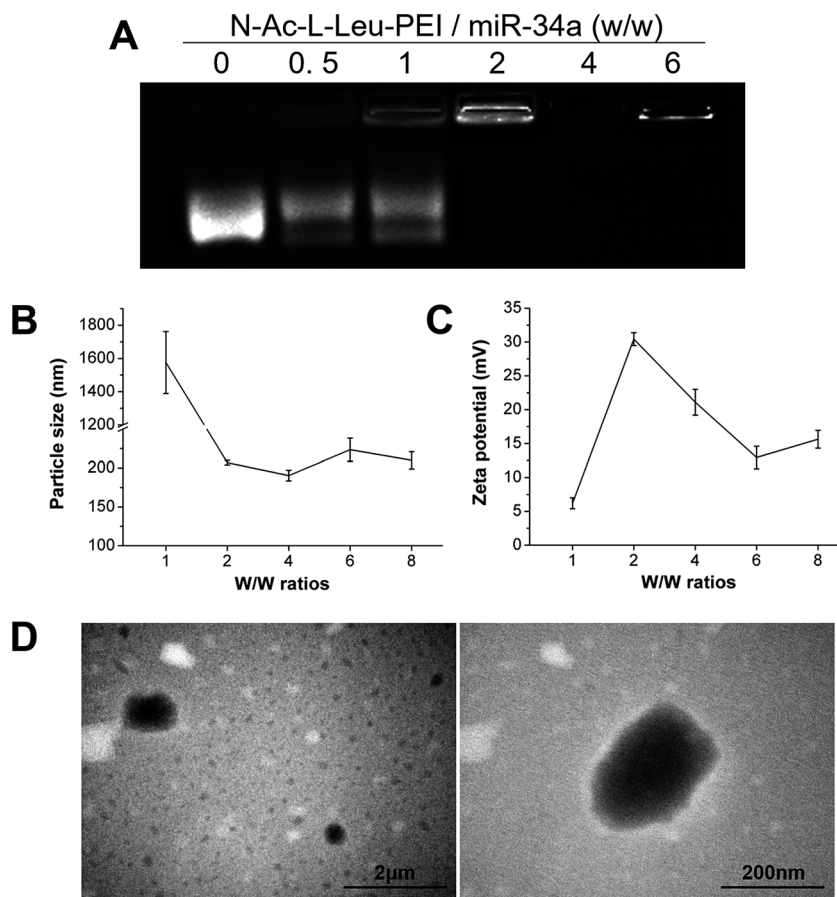


Fig. 1 Characteristics of *N*-Ac-L-Leu-PEI nanoparticles. The *N*-Ac-L-Leu-PEI/miR-34a nanocomplexes were prepared at different mass ratios for (A) agarose gel retardation assays, (B) particle size assays and (C) zeta potential assays, (D) TEM micrographs of *N*-Ac-L-Leu-PEI/miR-34a nanocomplexes with a mass ratio of 4 : 1. Data represent the means \pm SD of three independent experiments.

Lipofectamine 2000- and *N*-Ac-L-Leu-PEI-mediated transfection of FAM-miR-34a groups with 30–40% and 60–70% fluorescence intensity, respectively. FCM quantitative analysis of FAM-miR-34a⁺ cells revealed the highest positive rates in the *N*-Ac-L-Leu-PEI/miR-34a-FAM group to be at a w/w ratio of 4 (Fig. 2A). Moreover, qRT-PCR showed that 72 h after transfection of MG63 cells, *N*-Ac-L-Leu-PEI-mediated delivery of miR-34a produced a higher expression level of miR-34a (910 fold) compared with that for Lipofectamine 2000 (344 fold) (Fig. 2B). These data demonstrate that *N*-Ac-L-Leu-PEI can achieve high transfection efficiency and gene expression of miR-34a in cells, with an optimal mass ratio of 4.

3.3 Cytotoxicity of *N*-Ac-L-Leu-PEI *in vitro*

PEI has high cytotoxicity; therefore, Li²⁰ synthesized *N*-Ac-L-Leu-PEI by a 1-ethyl-3-(3-dimethylaminopropyl)-carbodiimide/*N*-hydroxysuccinimide (EDC/NHS)-mediated coupling reaction of *N*-acetyl-L-leucine on the primary amino group of PEI25K. This derivative has high resistance to protein adsorption and low hemolytic activity. In our MTT assay, the cell viability of three groups was more than 90%, and there was no cytotoxicity in either the Lipofectamine 2000/miR-34a group or the *N*-Ac-L-Leu-PEI/miR-34a group at 24, 48 and 72 h after transfection (Fig. 3A).

Similarly, further apoptosis assays (Fig. 3B) and live/dead cell viability assays (Fig. 4) revealed no significant influence of *N*-Ac-L-Leu-PEI on MG63 cells. *N*-Ac-L-Leu-PEI produced a slightly reduced population of early apoptotic cells and more live cells than Lipofectamine 2000. However, in group of PEI25K/miR-34a, the cell viability on 24, 48, 72 h was approximately 85%, 72%, 70%, respectively (Fig. 3), as well as elevated early and late cell apoptosis (23.54%) (Fig. 3) and red cells population in live/dead cell detection (Fig. 4). These results indicate that *N*-Ac-L-Leu-PEI owned lower toxicity of MG63 cells than PEI25K. We therefore considered *N*-Ac-L-Leu-PEI to be suitable for further transfection experiments and applications *in vitro* and *in vivo*.

3.4 Osteogenic differentiation of MG63 cells *in vitro*

Several recent reports have suggested that miR-34a is involved in the regulation of bone homeostasis. However, the reported roles of miR-34a in osteogenesis are not consistent, with some *in vitro* studies indicating a positive effect^{4,6} and some a negative effect.^{3,4} Most *in vivo* studies, showed up-regulation of miR-34a during osteogenesis. To determine whether miR-34a induces osteogenic differentiation of MG63 cells *in vitro*, we evaluated the early secretion function, and gene expression and protein levels during osteogenic differentiation. The early function



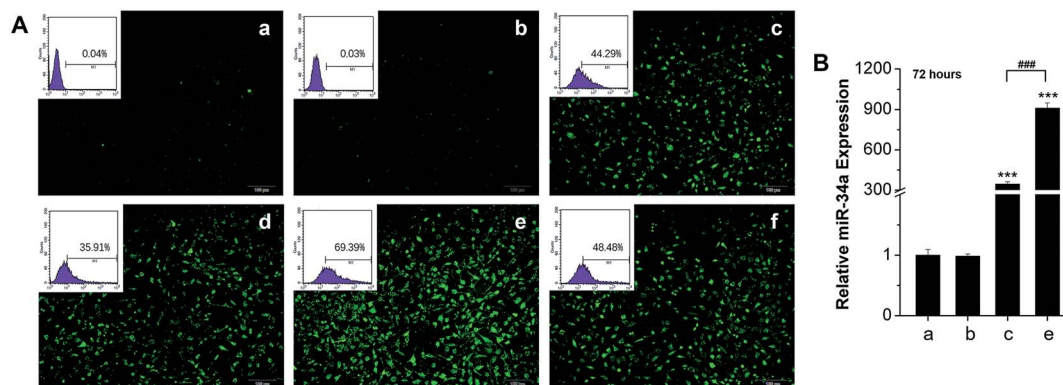


Fig. 2 Transfection efficiency of *N*-Ac-L-Leu-PEI/miR-34a. (A) Images of FAM-miR-34a-positive MG63 cells under fluorescent light and FCM. Scale bar: 100 μ m. (a) Blank, (b) FAM-miR-34a, (c) Lipofectamine 2000/FAM-miR-34a, (d) *N*-Ac-L-Leu-PEI/FAM-miR-34a with a w/w ratio of 2, (e) *N*-Ac-L-Leu-PEI/FAM-miR-34a with a w/w ratio of 4, (f) *N*-Ac-L-Leu-PEI/FAM-miR-34a with a w/w ratio of 6. (B) Real time PCR assay to examine the expression level of miR-34a in the 72 h after transfection. Data represent the means \pm SD of three independent experiments. * P < 0.05 vs. the blank group by paired t -test, # P < 0.05 vs. the Lipofectamine 2000/FAM-miR-34a group by paired t -test.

assay showed that miR-34a markedly improved ALP activity of MG63 cells at 24, 48 and 72 h after transfection (Fig. 5A) and that *N*-Ac-L-Leu-PEI-mediated miR-34a delivery led to significantly superior ALP activity augmentation compared with Lipofectamine 2000. The expression of *Runx2*, *SP7*, and *Col1* is related to osteoblastogenesis and is required for osteoblast differentiation.^{25–29} Gene expression and protein levels for *Runx2*, *SP7* and *Col1* were clearly elevated in miR-34a groups. The effect of miR-34a on genes and proteins of osteogenic differentiation (except for *Col1* mRNA levels) was greater with

N-Ac-L-Leu-PEI delivery compared with Lipofectamine 2000 delivery (Fig. 5B–D).

Our data clearly indicate that miR-34a elevates osteogenic differentiation of MG63 cells. This is in agreement with Grilli *et al.*, who confirmed osteogenic differentiation of osteosarcoma by miR-34a.³⁰ Moreover, compared with the commercial reagent, Lipofectamine 2000, *N*-Ac-L-Leu-PEI promoted higher levels of miR-34a-mediated osteogenic differentiation at the gene and protein expression levels and in early function.

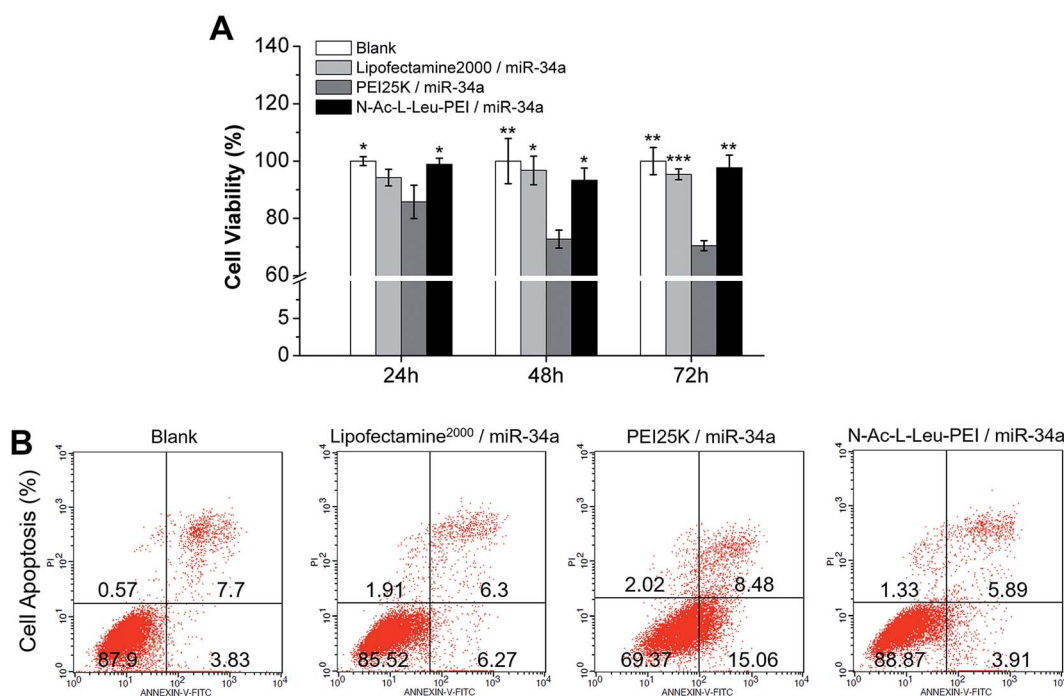


Fig. 3 Cytotoxicity of *N*-Ac-L-Leu-PEI in MG63 cells. (A) Cell viability of MG63 cells treated with the PEI25K/miR-34a nanocomplex (wt/wt, 4 : 1), *N*-Ac-L-Leu-PEI/miR-34a nanocomplex (wt/wt, 4 : 1) or Lipofectamine 2000/miR-34a for 24, 48 and 72 h. (B) Apoptosis of MG63 cells treated with the PEI25K/miR-34a nanocomplex (wt/wt, 4 : 1), *N*-Ac-L-Leu-PEI/miR-34a nanocomplex (wt/wt, 4 : 1) or Lipofectamine 2000/miR-34a for 72 h. Data represent the means \pm SD of three independent experiments. * P < 0.05 vs. the PEI25K/miR-34a group by paired t -test.



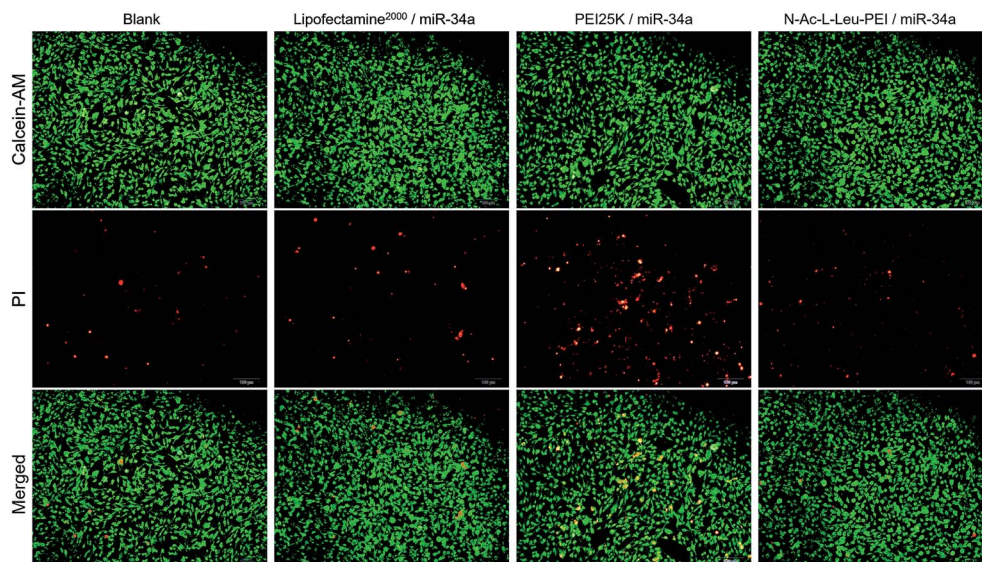


Fig. 4 Cytotoxicity of *N*-Ac-L-Leu-PEI in MG63 cells. Live/dead cell viability assay of MG63 cells treated with the PEI25K/miR-34a nanocomplex (wt/wt, 4 : 1), *N*-Ac-L-Leu-PEI/miR-34a nanocomplex (wt/wt, 4 : 1) or Lipofectamine 2000/miR-34a for 72 h.

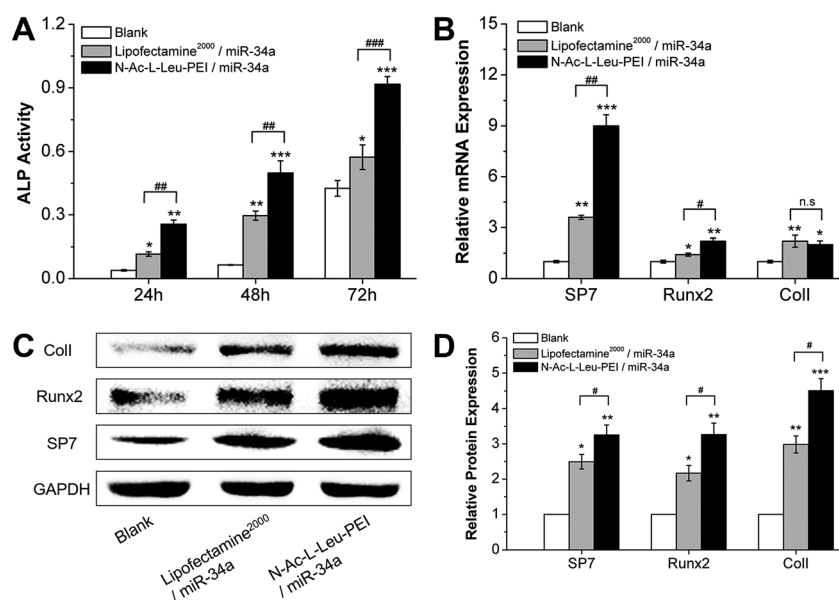


Fig. 5 Osteogenic differentiation of MG63 cells *in vitro*. (A) ALP activity assay of MG63 cells 24, 48 and 72 h post-transfection. (B) Quantitative real-time PCR analysis of *SP7*, *Runx2* and *Coll* mRNA levels 72 h post-transfection. (C and D) Western blot analysis (quality in C and quantity in D) of *SP7*, *Runx2* and *Coll* protein levels 72 h post-transfection. Data represent the means \pm SD of three independent experiments. * P < 0.05 vs. the blank group by paired *t*-test, # P < 0.05 vs. Lipofectamine 2000/miR-34a group by paired *t*-test.

3.5 Bone formation *in vivo*

We employed a rat cranial bone defect model to evaluate the *in vivo* regulation of *N*-Ac-L-Leu-PEI-mediated miR-34a delivery on bone formation. CBCT showed new bone formation to be rare, limited, and significantly increased in blank, Lipofectamine 2000/miR-34a and *N*-Ac-L-Leu-PEI/miR-34a groups, respectively (Fig. 6A). This was in accordance with the results of micro-CT. *N*-Ac-L-Leu-PEI-mediated miR-34a delivery clearly produced more new bone formation (61.79% new bone formation in the bone defect area) at 12 weeks post-implantation than Lipofectamine

2000-mediated miR-34a delivery (13.6% new bone formation in the bone defect area) (Fig. 6A and B). Moreover, significant augmentation of *Runx2*, *SP7* and especially *Coll* expression was observed in the *N*-Ac-L-Leu-PEI/miR-34a-treated bone defect area (Fig. 6C). Different from osteogenic differentiation *in vitro*, Lipofectamine 2000 failed to produce a new bone formation effect of miR-34a *in vivo*. These results indicate that *N*-Ac-L-Leu-PEI can deliver miR-34a to local tissues and that miR-34a retains the ability to promote new bone formation in an *in vivo* local bone defect model.



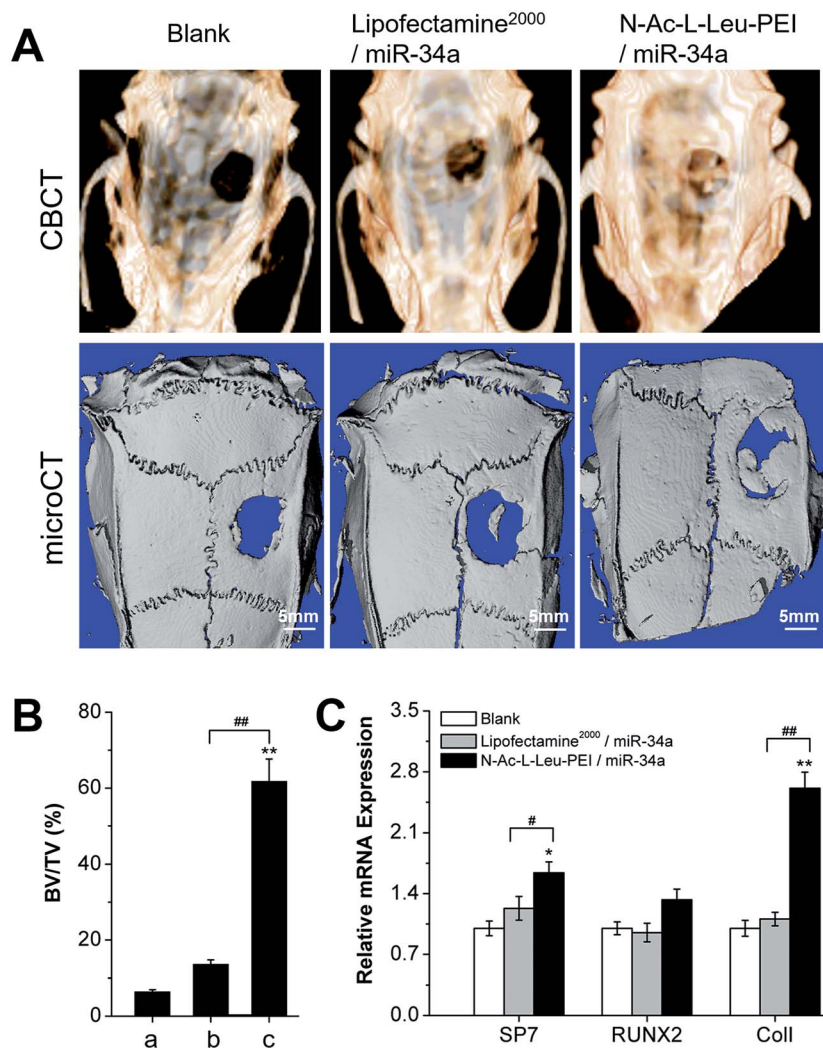


Fig. 6 Bone formation *in vivo* in a cranial bone defect model. (A) CBCT image and micro-CT analysis 12 weeks post-implantation. (B) Quantitative analysis of micro-CT new bone formation data in the bone defect area by Image-Pro Plus software. (a) blank, (b) Lipofectamine 2000/miR-34a, (c) *N*-Ac-L-Leu-PEI/miR-34a. (C) Quantitative real-time PCR analysis of *SP7*, *Runx2* and *Col1* mRNA levels in the cranial defect area 12 weeks post-implantation. Data represent the means \pm SD of three independent experiments. * P < 0.05 vs. the blank group by paired *t*-test, # P < 0.05 vs. Lipofectamine 2000/miR-34a group by paired *t*-test.

4. Discussion

Bone repair requires bone proliferation and differentiation to be continuously stimulated³¹ and the involvement of micro-RNAs in bone regeneration has been established. miR-34a has a prominent role in bone metabolism and has been employed in phase I clinical trials.³² In this article, we applied *N*-Ac-L-Leu-PEI to transport miR-34a with the aim to elevate its stability, cellular penetration and capability of promoting bone formation.

N-Ac-L-Leu-PEI possesses high resistance to protein adsorption, low hemolytic activity, low zeta potential and small particle size, as well as high transfection efficiency both in the presence and absence of FBS.²⁰ These characteristics make *N*-Ac-L-Leu-PEI suitable for forming stable nano-complexes and as a biocompatible gene delivery vehicle *in vitro*

and *in vivo*. In this study, we describe using *N*-Ac-L-Leu-PEI as an miR-34a carrier for stimulating MG63 cells *in vitro* and for local bone regeneration *in vivo*. *N*-Ac-L-Leu-PEI formed a stable nanocomplex with miR-34a and had high cellular uptake rates, superior to those of Lipofectamine 2000. Of note, *N*-Ac-L-Leu-PEI showed lower cytotoxicity than PEI25K, this can be explained as: the derivative *N*-Ac-L-Leu-PEI neutralized the excess positive charge of nanocomplex surface to induce less cell membrane disruption; *N*-Ac-L-Leu had lower non-specific protein adsorption capacity to improve the cell viability.²⁰ In addition, *N*-Ac-L-Leu-PEI not only delivered miR-34a into cells, but also released it to enable it to play a positive role in osteogenic differentiation *in vitro*. This was observed in the up-regulated expression of *Runx2*, *SP7* and *Col1* by qRT-PCR and western blotting and by ALP activity. *Runx2* is a bone differentiation factor,^{25,26} and *Runx2* activation in turn activates *SP7*



to launch osteogenic differentiation.^{27,28} ColI mainly provides a fibrous skeleton for the deposition of bone matrix.²⁸ ALP activity indicates the early secretion of bone tissue. Therefore, all the above are essential for bone formation. In addition, it was interesting to find that the *in vivo* effect of Lipofectamine 2000-mediated miR-34a delivery on osteogenesis was different to its *in vitro* effect. Because of complex microenvironments *in vivo*, carriers may easily be eliminated by immunological rejection or other reactions. Krzeszinski *et al.* obtained an approximately 5-fold increase in pre-miR-34a levels in bone marrow using chitosan nanoparticles after a single injection. Unfortunately, the osteogenesis promoted by miR-34a was insufficient to resist systemic bone loss in OVX mice and cancer bone metastases.⁴ Lipofectamine 2000 was unable to effectively deliver miR-34a to the bone defect area *in vivo*, while, miR-34a carried by *N*-Ac-L-Leu-PEI led to greater local bone formation. This was similar to the results of Fan *et al.* who demonstrated dramatic heterotopic bone formation in Bio-Oss collagen scaffolds.⁶ Our results indicate that *N*-Ac-L-Leu-PEI can protect miR-34a from degradation in complex *in vivo* environments.

5. Conclusions

The derivative *N*-Ac-L-Leu-PEI formed stable nanocomplexes with miR-34a and achieved high transfection efficiency without toxicity. Moreover, the carrier-mediated miR-34a delivery could trigger an effective promotion of osteogenic differentiation *in vitro* and new bone formation *in vivo*. miR-34 delivery by this PEI derivative signals a new gene therapy approach for bone regeneration.

Conflicts of interest

The authors declare no conflict of interest.

Acknowledgements

We thank Pro. Quanshun Li in Jilin University School of Life Sciences for providing the *N*-Ac-L-Leu-PEI. This research was supported by grants from the National Natural Science Foundation of China (No. 81371153), Jilin Natural Science Foundation (No. 20170311032YY, No. 20160101335JC), the Medical Support Program of the Jilin university (No. 470110000423) and Jilin provincial education department project (Ji jiao ke he zi [2016] No. 485).

References

- 1 U. Ripamonti and J. C. Petit, *Cytokine Growth Factor Rev.*, 2009, **20**, 489–499.
- 2 H. Kang, H. Chen, P. Huang, J. Qi, N. Qian, L. Deng and L. Guo, *Osteoporosis Int.*, 2016, **27**, 1493–1505.
- 3 L. Chen, K. Holmstrom, W. Qiu, N. Ditzel, K. Shi, L. Hokland and M. Kassem, *Stem Cells*, 2014, **32**, 902–912.
- 4 J. Y. Krzeszinski, W. Wei, H. Huynh, Z. Jin, X. Wang, T. C. Chang, X. J. Xie, L. He, L. S. Manqala, G. Lopez-Berestein, A. K. Sood, J. T. Mendell and Y. Wan, *Nature*, 2014, **512**, 431–435.
- 5 J. Wei, Y. Shi, L. Zheng, B. Zhou, H. Inose, J. Wang, X. E. Guo, R. Grosschedl and G. Karsenty, *J. Cell Biol.*, 2012, **197**, 509–521.
- 6 C. Fan, L. Jia, Y. Zheng, C. Jin, Y. Liu, H. Liu and Y. Zhou, *Stem Cell Rep.*, 2016, **7**, 236–248.
- 7 M. Wan, B. Gao, F. Sun, Y. Tang, L. Ye, Y. Fan, O. D. Klein, X. Zhou and L. Zheng, *PLoS One*, 2012, **7**, e50090.
- 8 F. Sun, M. Wan, X. Xu, B. Gao, Y. Zhou, J. Sun, L. Cheng, O. D. Klein, X. Zhou and L. Zheng, *J. Dent. Res.*, 2014, **93**, 589–595.
- 9 G. Lambert, E. Fattal and P. Couvreur, *Adv. Drug Delivery Rev.*, 2001, **47**, 99–112.
- 10 D. W. Pack, A. S. Hoffman, S. Pun and P. S. Stayton, *Nat. Rev. Drug Discovery*, 2005, **4**, 581–593.
- 11 M. A. Mintzer and E. E. Simanek, *Chem. Rev.*, 2009, **109**, 259–302.
- 12 K. Xiu, J. J. Yang, N. N. Zhao, J. S. Li and F. J. Xu, *Acta Biomater.*, 2013, **9**, 4726–4733.
- 13 A. E. Nel, L. Madler, D. Velegol, T. Xia, E. M. Hoek, P. Somasundaran, F. Klaessiq, V. Castranova and M. Thompson, *Nat. Mater.*, 2009, **8**, 543–557.
- 14 Z. ur Rehman, D. Hoekstra and I. S. Zuhorn, *ACS Nano*, 2013, **7**, 3767–3777.
- 15 D. Fischer and Y. Li, *Biomaterials*, 2003, **24**, 1121–1131.
- 16 A. M. Funhoff, C. F. van Nostrum, M. C. Lok, M. M. Fretz, D. J. Crommelin and W. E. Hennink, *Bioconjugate Chem.*, 2004, **15**, 1212–1220.
- 17 H. Tian, W. Xiong, J. Wei, Y. Wang, X. Chen, X. Jing and Q. Zhu, *Biomaterials*, 2007, **28**, 2899–2907.
- 18 H. Tian, F. Li, J. Chen, Y. Huang and X. Chen, *Macromol. Biosci.*, 2012, **12**, 1680–1688.
- 19 Z. Guo, H. Tian, L. Lin, J. Chen, C. He, Z. Tang and X. Chen, *Macromol. Biosci.*, 2014, **14**, 1406–1414.
- 20 Z. Li, L. Zhang and Q. Li, *Colloids Surf., B*, 2015, **135**, 630–638.
- 21 Z. Xing, S. Gao, Y. Duan, H. Hao, L. Li, Y. Yang and Q. Li, *Int. J. Nanomed.*, 2015, **10**, 5715–5727.
- 22 Y. Zheng, C. Lin, X. Hou, *et al.*, *RSC Adv.*, 2017, **7**, 27121–27127.
- 23 H. Yin, L. Cui and Y. Cao, *Chin. J. Aesthetic Med.*, 2009, **18**, 727–729.
- 24 L. Zhao, K. Zhang, W. H. Bu, X. W. Xu, H. Jin, B. Chang, B. C. Wang, Y. J. Sun, B. Yang, C. Y. Zheng and H. C. Sun, *RSC Adv.*, 2016, **41**, 34081–34089.
- 25 K. Redlich and J. S. Smolen, *Nat. Rev. Drug Discovery*, 2012, **11**, 234–250.
- 26 Y. Zhang, R. Xie, C. M. Croce, J. L. Stein, J. B. Lian, A. J. van Wigen and G. S. Stein, *Proc. Natl. Acad. Sci. U. S. A.*, 2011, **108**, 9863–9868.
- 27 X. Zhou, Z. Zhang, J. Q. Feng, V. M. Dusevich, K. Sinha, H. Zhang, B. G. Darnay and B. de Crombrughe, *Proc. Natl. Acad. Sci. U. S. A.*, 2010, **10**, 12919–12924.
- 28 K. Nakashima, X. Zhou, G. Kunkel, Z. Zhang, J. M. Deng, R. R. Behringer and B. de Crombrughe, *Cell*, 2002, **108**, 17–29.



- 29 E. Hesse, T. E. Hefferan, J. E. Tarara, C. Haasper, R. Krettek, L. Lu and M. J. Yaszemski, *J. Biomed. Mater. Res., Part A*, 2010, **94**, 442–449.
- 30 A. Grilli, M. Sciandra, M. Terracciano, P. Picci and K. Scotlandi, *BMC Med. Genomics*, 2015, **8**, 34.
- 31 K. Andreas, R. Zehbe, M. Kazubek, K. Grzeschik, N. Sternberg, H. Baumler, H. Schubert, M. Sittinger and J. Ringe, *Acta Biomater.*, 2011, **7**, 1485–1495.
- 32 M. Agostini and R. A. Knight, *OncoTargets Ther.*, 2014, **5**, 872.

